Electronic Supplementary Information

Enhanced activity of electrocatalytic hydrogen evolution reaction by 2D/2D nanohybrids of ruthenate nanoflakes and graphitic carbon nitride

Takayuki Ban*, Kazuki Inukai, Chika Takai-Yamashita, and Kazuhiro Manseki

Department of Chemistry and Biomolecular Science, Gifu University, Yanagido 1-1, Gifu 501-1193, Japan

Corresponding author [*]: ban.takayuki.z6@f.gifu-u.ac.jp

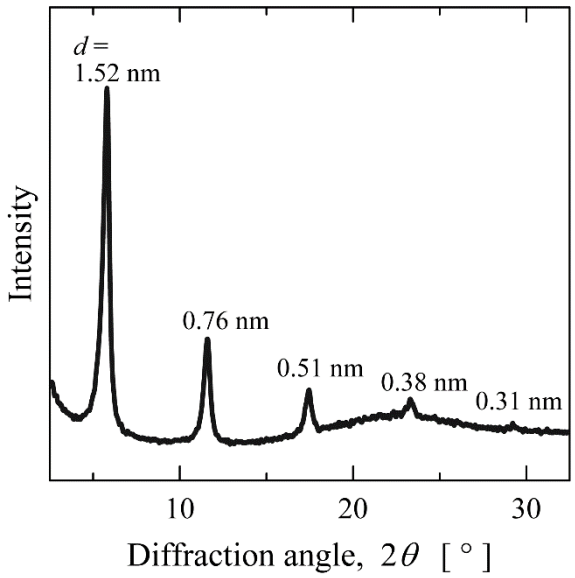

Figure S1 XRD pattern of the thin film fabricated by drop-casting the aqueous sol of ruthenate nanoflakes on a glass substrate

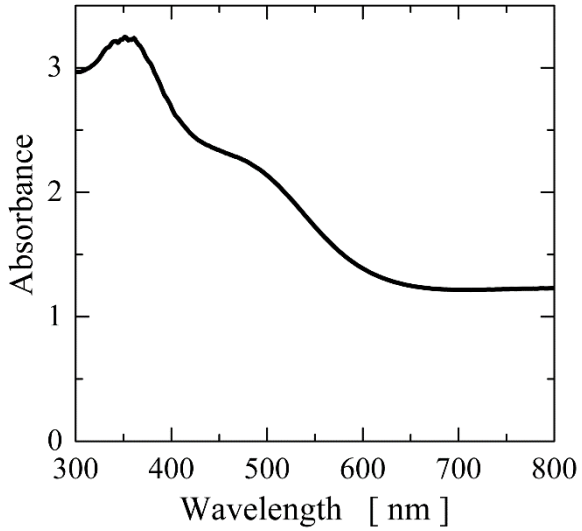

Figure S2 UV-vis spectrum of the aqueous sol of ruthenate nanoflakes

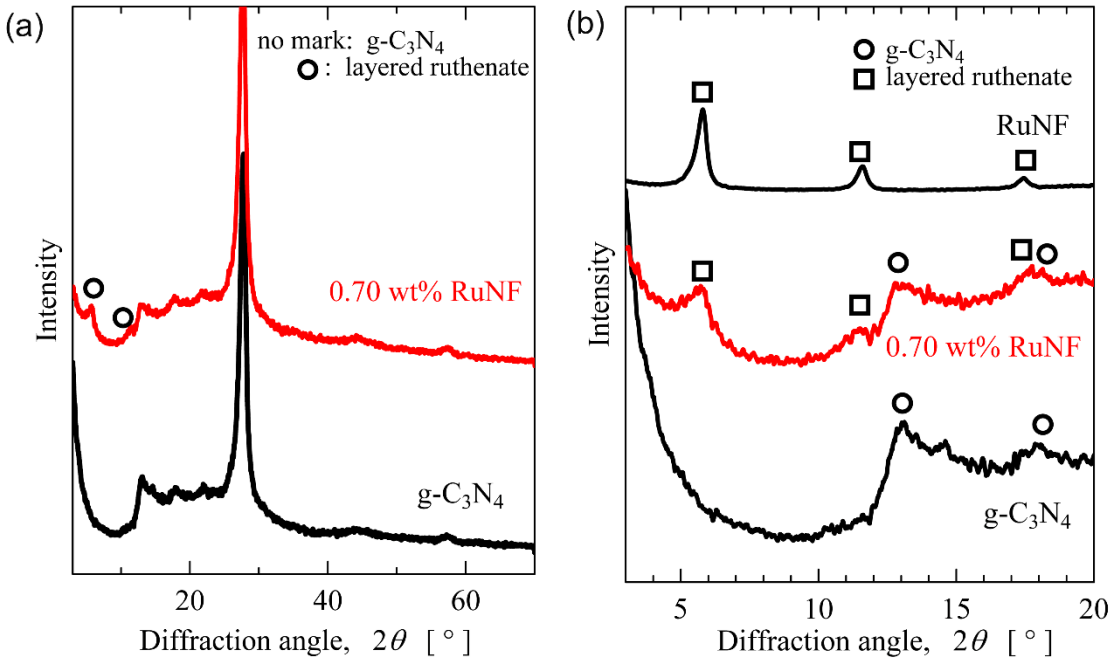

Figure S3 XRD patterns of RuNF/ g-C_3N_4 hybrid (0.70 wt% RuNF) and g-C_3N_4 before washing with 2-propanol

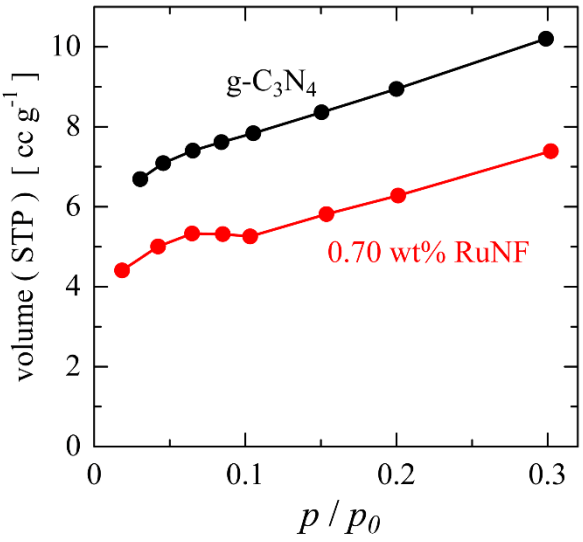

Figure S4 Isotherms of N_2 adsorption at 77 K for g-C_3N_4 powder and RuNF/ g-C_3N_4 hybrid with a RuNF content of 0.70 wt%

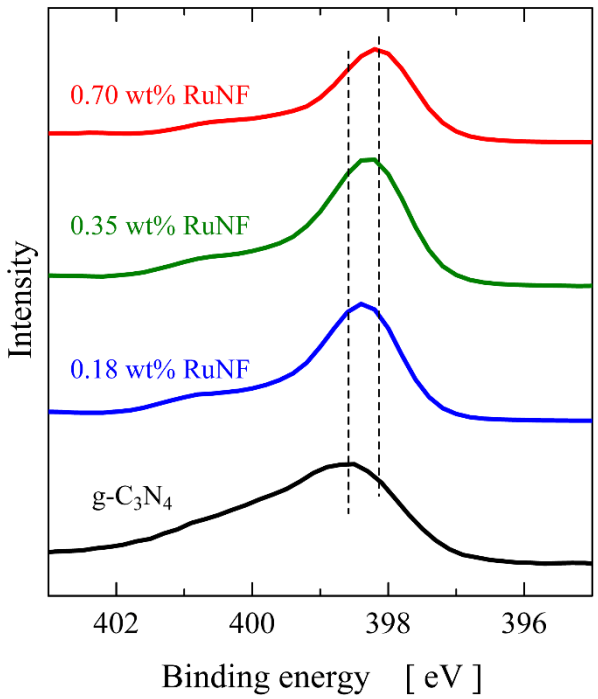

Figure S5 XPS N1s spectra of g-C_3N_4 powder and RuNF/ g-C_3N_4 hybrids with RuNF contents of 0.18, 0.35, and 0.70 wt%. The vertical broken lines correspond to binding energies of 398.2 and 398.6 eV.

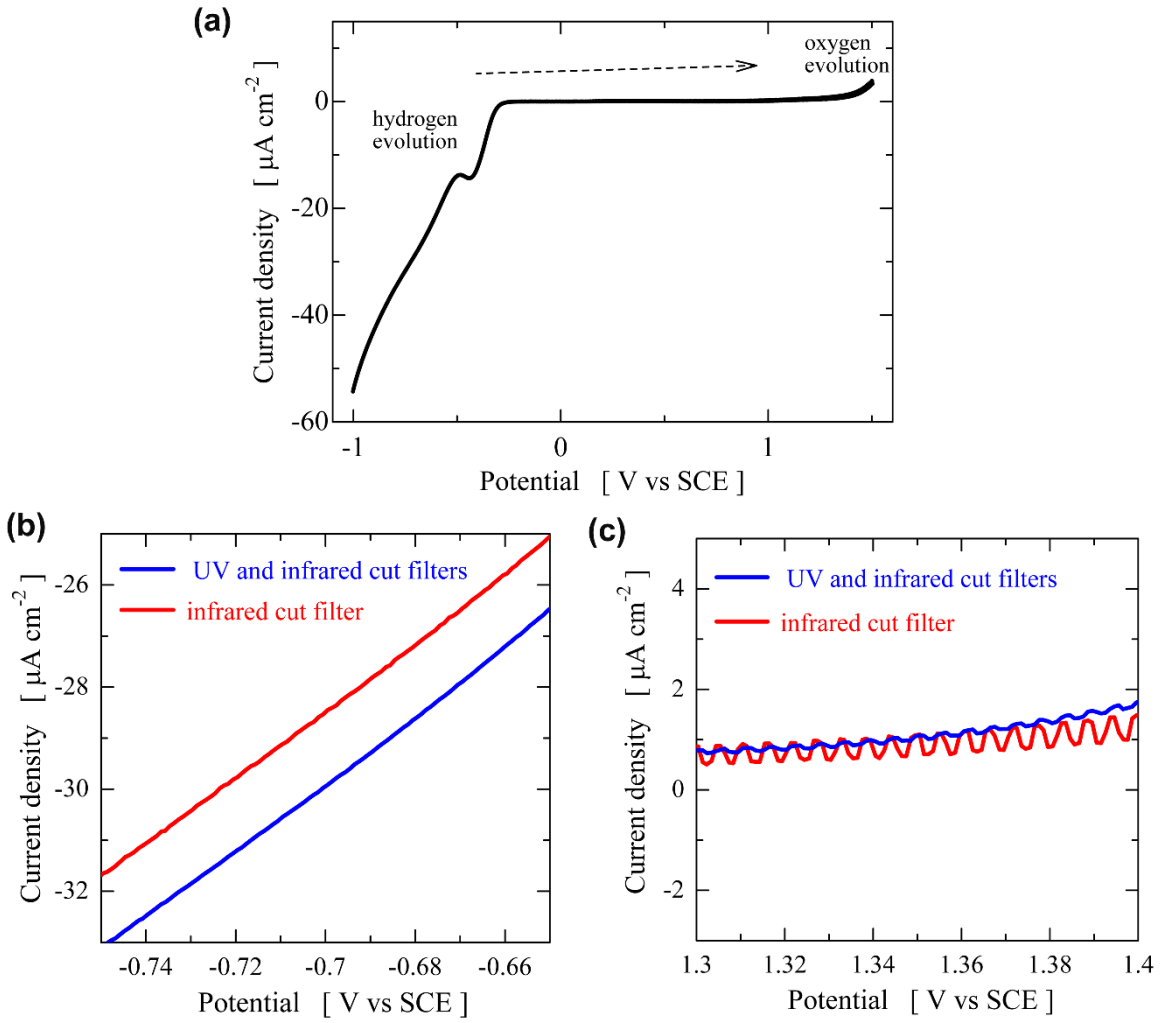

Figure S6 (a) Change of current density with potential for the electrolysis of 0.1 M Na_2SO_4 aqueous solution using FTO film without coating as a work electrode. The electrode was irradiated by intermittent light passed through infrared-cut filter. The applied potential was changed from -1 V to 1.5 V vs SCE. Panels (b) and (c) show the current density change in the potential ranges where hydrogen and oxygen evolution reactions occurred, respectively, for using the lights passed through infrared-cut filter and through both infrared-cut and UV-cut filters.

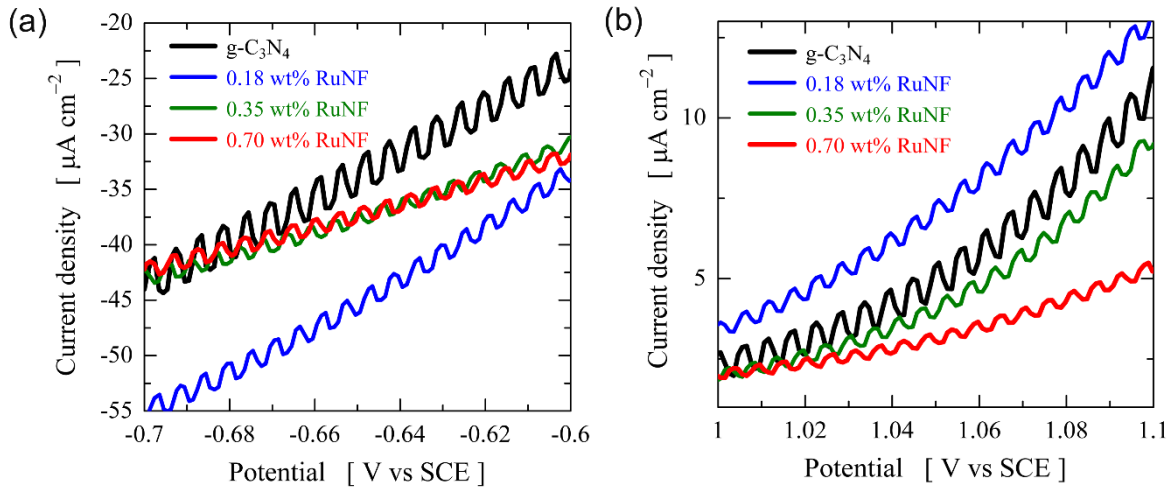

Figure S7 Change of current density with potential for the electrolysis of 0.1 M Na_2SO_4 aqueous solution with an intermittent irradiation of the light passed through both the infrared-cut and UV-cut filters. RuNF/ g-C_3N_4 hybrids with different RuNF contents, i.e., 0, 0.18, 0.35, and 0.70 wt% RuNF, were used as a working electrode. The applied potential was changed from -1 V to 1.5 V vs SCE. Panels (a) and (b) show the current density changes in the potential ranges where hydrogen and oxygen evolution reactions occurred, respectively.

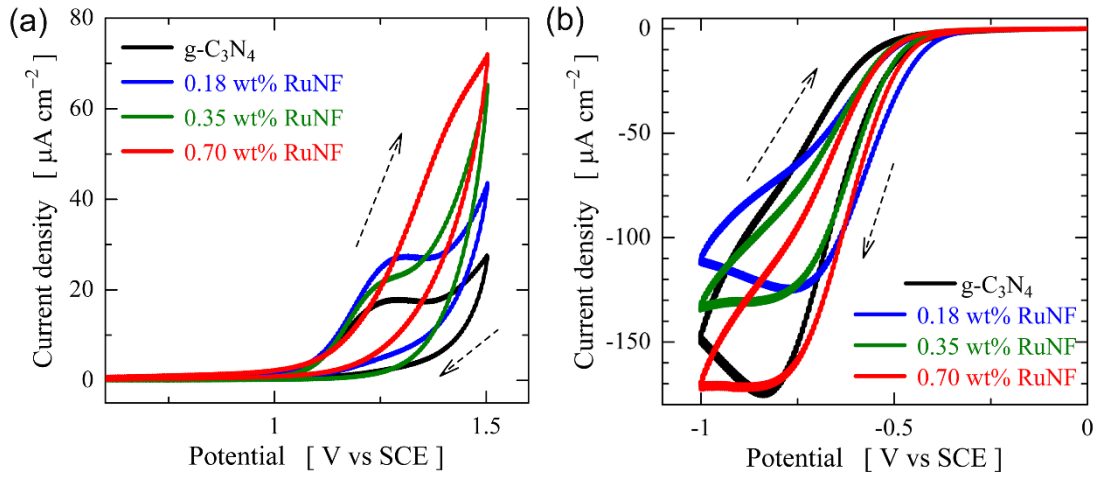

Figure S8 Cyclic voltammograms of the electrolysis of 0.1 M Na_2SO_4 aqueous solution using RuNF/ g-C_3N_4 hybrids with different RuNF contents, i.e., 0, 0.18, 0.35, and 0.70 wt% RuNF, as a working electrode. Panels (a) and (b) show the current density changes in the potential ranges where oxygen and hydrogen evolution reactions occurred, respectively.

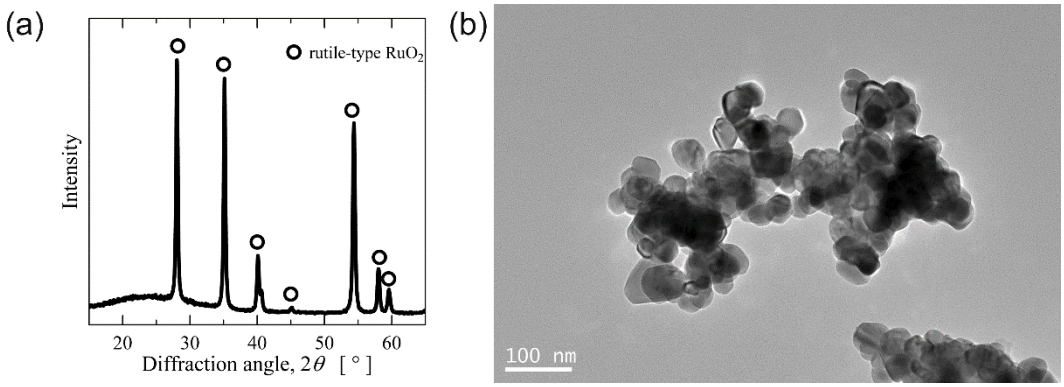

Figure S9 (a) XRD pattern and (b) TEM image of the RuO_2 nanoparticles used for comparison with RuNFs

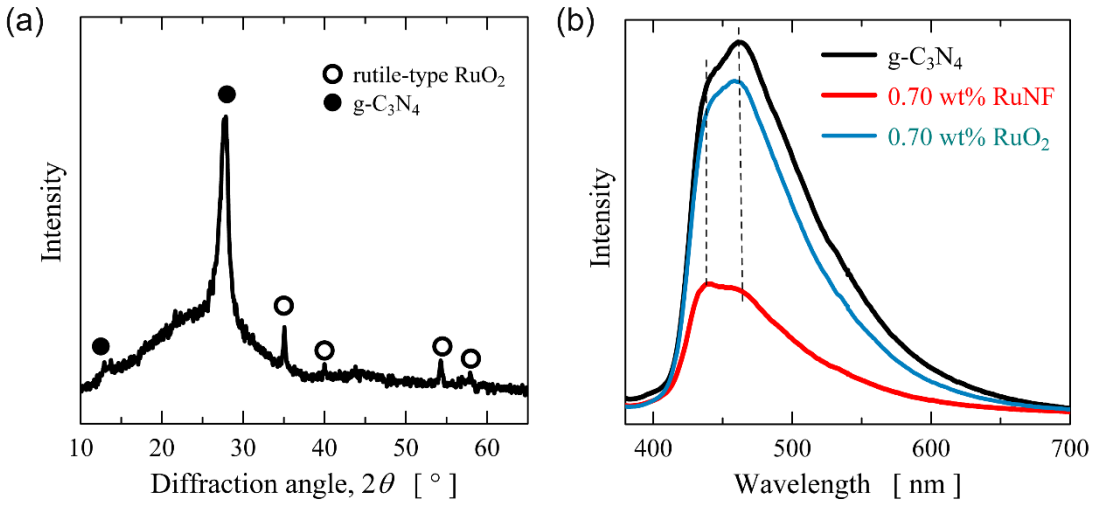

Figure S10 (a) XRD pattern and (b) fluorescence spectrum of RuO_2 particle/ g-C_3N_4 hybrid with a RuO_2 content of 0.70 wt%. The fluorescence spectrum was measured with an excitation wavelength of 370 nm. For comparison, the fluorescence spectra of RuNF/ g-C_3N_4 hybrid with a RuNF content of 0.70 wt% and g-C_3N_4 are also shown in the panel (b).

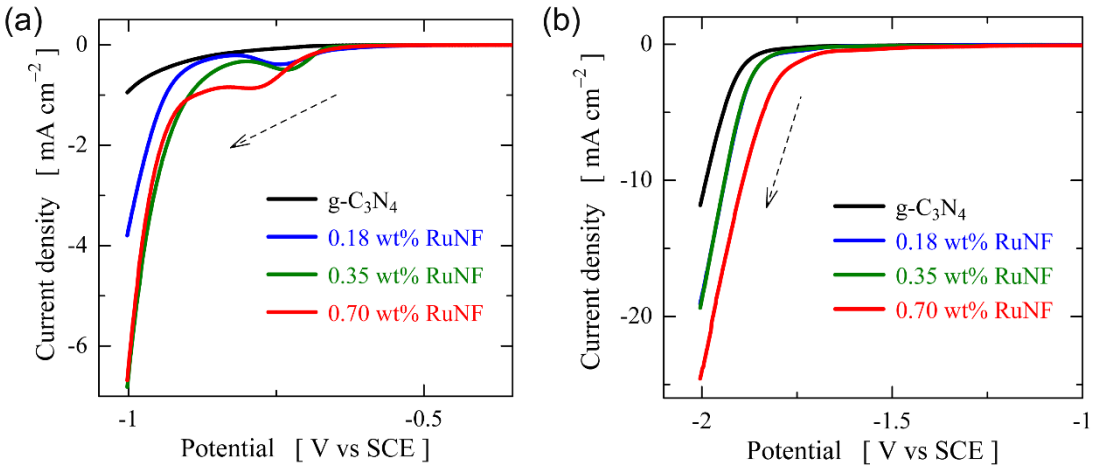

Figure S11 Current density changes by hydrogen evolution reaction in (a) 0.5 M H_2SO_4 aqueous solution and (b) 0.5 M NaOH aqueous solution by using RuNF/ g-C_3N_4 hybrids with different RuNF contents, i.e., 0, 0.18, 0.35, and 0.70 wt% RuNF, as a working electrode.